

# Dark Matter Signatures of Supermassive Black Hole Binaries

Smadar Naoz\*

*Department of Physics and Astronomy, University of California, Los Angeles, CA 90095, USA.  
Mani L. Bhaumik Institute for Theoretical Physics, UCLA, Los Angeles, CA 90095, USA*

Joseph Silk

*Institut d'Astrophysique de Paris, UMR 7095 CNRS,  
Sorbonne Universités, 98 bis, boulevard Arago, F-75014, Paris, France  
The Johns Hopkins University, Department of Physics and Astronomy, Baltimore, Maryland 21218, USA  
Becroft Institute of Particle Astrophysics and Cosmology, University of Oxford, Oxford OX1 3RH, UK*

A natural consequence of the galaxy formation paradigm is the existence of supermassive black hole (SMBH) binaries. Gravitational perturbations from a massive far away SMBH can induce high orbital eccentricities on dark matter particles orbiting the primary SMBH, via the eccentric Kozai-Lidov mechanism. This process yields an influx of dark matter particles into the primary SMBH ergosphere, where test particles linger for long timescales. This influx results in high self-gravitating densities, forming a dark matter clump extremely close to the SMBH. In such a situation, the gravitational wave emission between the dark matter clump and the SMBH is potentially detectable by LISA. If dark matter self-annihilates, the high densities of the clump will result in a unique co-detection of gravitational wave emission and high energy electromagnetic signatures.

## I. INTRODUCTION

The hierarchical nature of the galaxy formation paradigm suggests that major galaxy mergers may result in the formation of supermassive black hole (SMBH) binaries [1–4]. While observations of SMBH binaries are challenging, there are several confirmed systems and observed binary candidates with sub-parsec to tens to hundreds of parsec separations [e.g., 5–19]. Furthermore, several observations of active galactic nuclei pairs with kpc-scale separations have been suggested as SMBH binary candidates [e.g., 20–26]. Numerical experiments for spheroidal gas-poor galaxies suggest that these binaries can reach parsec separation and may stall there [e.g., 27–29].

While the Dark Matter (DM) distribution in galaxies was studied extensively in the literature, the DM profile for sub-kpc scales is largely unknown. In Naoz & Silk (2014) [Ref. 30], we suggested that gravitational perturbations in SMBH binaries can have important implications for the DM distribution around the *less* massive member of the binary. The requirement that the perturbing SMBH will be more massive than the primary arises from the need to overcome general relativistic precession of the DM particle orbits [31]. Gravitational perturbations from a far-away SMBH, on a DM particle orbiting around the SMBH primary can result in extremely high eccentricities due to a physical process known as the “Eccentric Kozai-Lidov” (EKL) mechanism [32]. The eccentricities can reach extreme values [33] such that the pericenter passage of the DM particle reaches the SMBH ergosphere (or even the event horizon) [30]. This process results in a DM torus-like configuration around the

less massive SMBH [30]. These surviving particles were initially in a less favorite EKL regime of the parameter space, compared to those that reached high eccentricities.

The low-energy, low angular momentum orbit of a test particle around a spinning black hole has been addressed in the literature upto 4th order in the post-Newtonian approximation [34], and may yield an increase of the DM density around a rotating SMBH [35]. The EKL mechanism in SMBH binary systems results in extremely low angular momentum orbits of the DM particle [30], eventually decoupled from the companion SMBH and accumulating in the vicinity of the primary SMBH.

Here we show that the accumulation of DM in the ergosphere of an SMBH can reach such high densities as to allow for formation of self-gravitating DM clumps. Such a clump then emits a gravitational wave (GW) emission signal, potentially detectable by LISA, while possibly undergoing self-annihilation. This process may yield a unique co-signal of GW emission and high energy electromagnetic signature arising from the self-annihilation process of DM.

## II. SELF-GRAVITATING DM CLUMPS

DM is expected to be inhomogenous and clumpy [36–38]. This clumpy nature can be explained as a simple extrapolation to very small scales of the primordial power spectrum, and in large parts of the Universe these clumps are expected to be free from gas [39–42]. Furthermore, some DM clumps may have formed shortly after or during radiation-matter equality due to phase transitions, topological defects, or collapse into primordial perturbations [37, 43, 44]. Moreover, these clumps may have formed at earlier epochs due to accretion onto primordial black holes [45]. Regardless of their formation mechanism, these clumps need to be self-gravitating in order to

---

\* snaoz@astro.ucla.edu

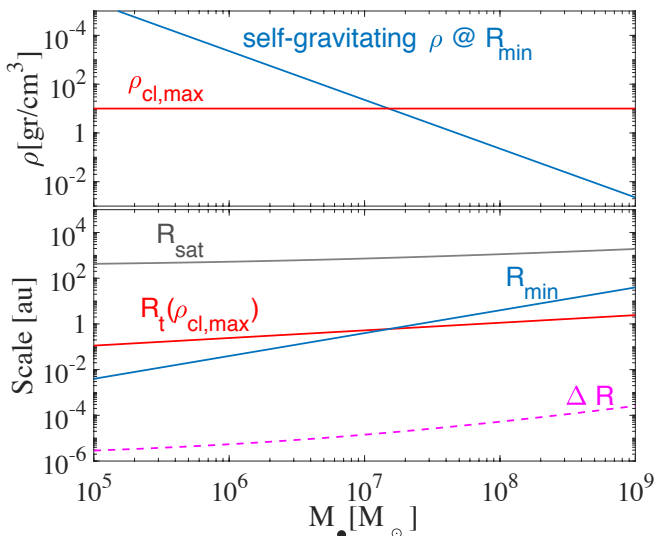


FIG. 1. **Typical density and physical scales in the system.** *Top panel:* we consider the self-gravitating density required at  $R_{\min}$  (blue line). We also show (red, horizontal line) the maximum clump density for a self-gravitating, self-annihilating DM clump within a dynamical time scale (adopting  $m_\chi = 100$  GeV DM particle). *Bottom panel:* relevant physical scales in the system. We consider the ergosphere scale,  $R_{\min}$  (Eq. (2)), as well as the tidal radius,  $R_t$ , (Eq. 1), for  $\rho_{\text{cl}} = \rho_{\text{cl,max}}$ . We also show the typical “thickness” scale of the self-gravitating clump,  $\Delta R$ , see text.

resist disruption from other objects in the Universe.

In the vicinity of a SMBH with a mass  $M_\bullet$ , we define the tidal radius, at which the gravitational tidal field of the SMBH overcomes the DM clump self-gravity:

$$R_t \sim \left( \frac{3M_\bullet}{4\pi\rho_{\text{cl}}} \right)^{1/3}, \quad (1)$$

where  $\rho_{\text{cl}}$  is the density of the DM clump. In Naoz & Silk, we showed that gravitational perturbations forming a distant SMBH can develop high eccentricity excitations to the DM particle orbits reaching all the way to the ergosphere radius. The latter is estimated as (depicted in the bottom panel of Figure 1) :

$$R_{\min} = \frac{4GM_\bullet}{c^2}, \quad (2)$$

where  $c$  is the speed of light and  $G$  is the gravitational constant. We find the critical density for a self-gravitating clump at the ergosphere by setting  $R_{\min} = R_t$ . In other words,

$$\rho_{\text{SG}} = \frac{3}{256\pi} \frac{c^6}{G^3 M_\bullet^2}. \quad (3)$$

This critical density is depicted in Figure 1, top panel.

Assuming that DM self-annihilates places an upper limit on the DM density of a clump by requiring that

the clump does not self-annihilate within a given time  $t$ . In other words:

$$\rho_{\text{cl}} \lesssim \frac{m_\chi}{\langle\sigma v\rangle t}, \quad (4)$$

where  $\langle\sigma v\rangle$  is the thermal velocity-averaged annihilation cross-section times the particle velocity,  $m_\chi$  is the mass of the DM particle. Considering the DM distribution in galaxies, the relevant time-scale is typically the age of the system, which results in a saturated core density,  $\rho_{\text{sat}}$ , at the center of a galaxy [46–48]. Here we adopt the dynamical timescale,  $t_D$ , of the self-gravitating clump [49], that describes a significant change to the clump due to its own gravity

$$t_D = \sqrt{\frac{3}{4\pi G \rho_{\text{cl}}}}. \quad (5)$$

Thus, setting the time in Equation (4) to be the above dynamical time, we can obtain an upper limit on the clump’s density, for self-annihilating, self-gravitating clumps

$$\rho_{\text{cl,max}} \sim \frac{4\pi G}{3} \left( \frac{m_\chi}{\langle\sigma v\rangle} \right)^2. \quad (6)$$

In Figure 1, we show this upper limit for  $m_\chi = 100$  GeV DM particles and adopting the canonical velocity-averaged annihilation cross-section times velocity  $\langle\sigma v\rangle = 3 \times 10^{-26} \text{ cm}^3 \text{ s}^{-1}$  [50].

From the comparison between  $\rho_{\text{SG}}$  and  $\rho_{\text{cl,max}}$ , we find a minimum SMBH mass that can allow formation of a self-gravitating spherical clump:

$$M_{\bullet,\text{lim}} \sim \frac{3}{32\pi} \frac{c^3 \langle\sigma v\rangle}{G^2 m_\chi}. \quad (7)$$

For  $m_\chi = 100$  GeV DM particles, we find  $M_{\bullet,\text{lim}} \sim 1.5 \times 10^7 M_\odot$ . This is the mass at the crossing point between  $\rho_{\text{SG}}$  and  $\rho_{\text{cl,max}}$ , depicted in Figure 1. Larger DM mass particles will result in smaller limiting masses. We stress that the above scaling corresponds to spherical symmetry which is not an accurate representation of the configuration of this system, and thus this limit should be treated as an order-of-magnitude estimate.

### III. ACCUMULATION AND ANNIHILATION OF DM

Naoz & Silk pointed out that DM particles are accumulated into the vicinity of the ergosphere of an SMBH, due to the gravitational perturbations from a companion that is a far-away SMBH, i.e. via the aforementioned EKL mechanism. As the DM particles accumulate on the ergosphere, they may reach self-gravitating densities. Therefore, the accumulated mass as a function of the time  $M_{\text{acc}}$ , due to the EKL mechanism of the system,

can be estimated from the dynamical simulations presented in Naoz & Silk (2014). In that work, we showed that the accumulation rate as a function of time has similar time dependency for different SMBH primaries (this is an expected result from the EKL mechanism [32]). We thus adopt this time dependence for an assumed DM distribution upto the SMBH sphere of influence.

Gondolo & Silk (1999) [Ref. 46] showed that the distribution of DM can be enhanced around the centers of galaxies, at a radius which is at the order of the SMBH sphere of influence. We thus adopt the following density profile, inwards of the sphere of influence [46],

$$\rho_{DM} = \begin{cases} 0 & r \leq 2GM_{\bullet}/c^2, \\ \rho_{\text{sat}} & 2GM_{\bullet}/c^2 < r \leq R_{\text{sat}}, \\ \rho_{\text{sat}} \left(\frac{r}{R_{\text{sat}}}\right)^{-\gamma} & R_{\text{sat}} < r \leq R_{\text{spike}}, \end{cases} \quad (8)$$

and assume a NFW profile for  $r > R_{\text{spike}}$ . The latter can be then connected to different SMBH masses via the  $m - \sigma$  relation [51]. From Eq. (4), the saturated density is  $\rho_{\text{sat}} = m_x / (\langle \sigma v \rangle t_{\bullet})$ , where we adopt  $t_{\bullet} = 10^{10}$  yr as the age of the SMBH. The power-law index  $\gamma$  is expected to be between 2.25 – 2.5 [52], and in what follows we adopt  $\gamma = 7/3$  [53]. Demanding continuation between the different profile segments, we find the spike radius,  $R_{\text{spike}}$ , and the saturated radius,  $R_{\text{sat}}$ , (shown in bottom panel of Figure 1).

The DM mass accumulation as a function of time is depicted in Figure 2, top panel. As shown in this Figure, for about  $10^8$  yr, there is continued accumulation of mass onto the ergosphere. The total mass accumulated (integrated over time), is about 15% of the mass in the sphere of influence due to the EKL mechanism [30]. Note that this is a lower limit, which take into account the possibility of high eccentric particles that are captured by the massive SMBH perturber [54], but can be as high as  $\sim 50\%$  if the perturber SMBH grows in mass [30].

The height scale associated with the mass that accumulated in the vicinity of the SMBH is on the order of  $\Delta R = \eta GM_{\text{acc}}/c^2$ , where  $\eta > 2$  (to avoid a singularity). In Figure 1, we show  $\Delta R(\max[M_{\text{acc}}])$  found from the self-gravitating density over a volume of  $\sim 4\pi(2GM_{\bullet}/c^2)^2 \Delta R$ . For this case, we find that  $\eta = 16/3$ . Due to the deviations from spherical symmetry (smaller surface area) in the accumulated material, we expect  $\Delta R$  to be larger than depicted in Figure 1.

For annihilating DM particles, these high densities will undergo rapid annihilation. The annihilation timescale is estimated as

$$t_{\text{ann}} \sim \frac{m_x}{\rho_{\text{SG}} \langle \sigma v \rangle}, \quad (9)$$

shown as dotted lines in the bottom panel of Figure 2. We note that we use  $\rho_{\text{SG}}$  rather than  $\rho_{\text{cl,max}}$ , because the former represents the maximum density at which the clump self-gravity will overcome the SMBH tidal forces, irrespectively of self-annihilation. However, the strong gravitational field of the SMBH may affect the dynamics,

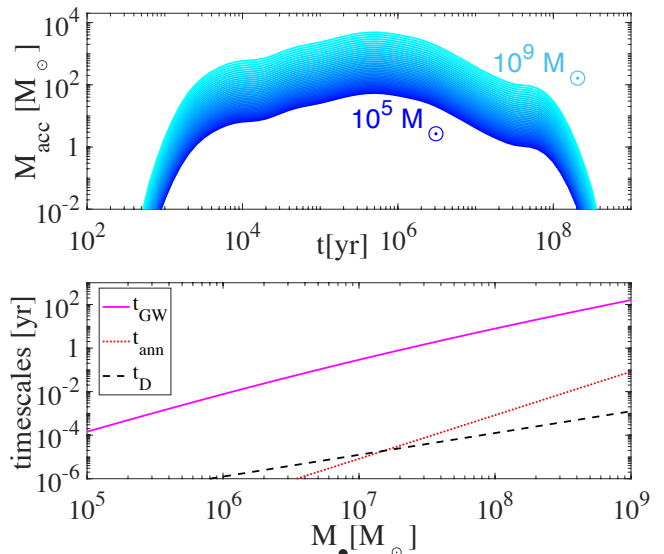


FIG. 2. **Top panel:** we consider the instantaneous accumulating mass at  $R_{\text{min}}$ , for a range of SMBH masses from  $10^9 M_{\odot}$  (cyan, top), to  $10^5 M_{\odot}$ , (blue, bottom). The time dependency is adopted from the Naoz & Silk dynamical simulations, for a density profile from Eq. (8). **Bottom panel:** the relevant time-scales in the problem. We show the GW time-scale, where we consider the maximum accumulated mass, and thus this is the shortest GW merger time-scale. We also consider the dynamical time-scale for a self-gravitating clump, Eq. (5), (which is independent of annihilation processes). This time-scale represents a significant change that a spherical clump undergoes due to its own gravity. Finally we consider the annihilation time-scale (Eq. (9)) which is much shorter than the GW merger timescale.

and thus, Equation (9) underestimates the annihilation timescale for masses below  $M_{\bullet,\text{lim}}$ . While the clump self-annihilates, the ergosphere accumulates more DM particles via the EKL mechanism (as depicted on Figure 2, top panel).

#### IV. GRAVITATIONAL WAVE EMISSION SIGNAL

The orbit of a self-gravitating clump will shrink due to gravitational wave (GW) emission. We estimate the merger timescale [55], although we note that the clump is not a point mass, on the other-hand, due to the EKL accumulation, it does not exhibit radial symmetry either. Below, we first estimate the mass for a clump at  $R_{\text{min}}$ , adopting the maximum accumulated mass (see Figure 2), thus having a lower limit on the merger timescale between the clump and the SMBH. As depicted in Figure 2, bottom panel, the merger timescale via GW emission is much longer than the annihilation timescale. Thus, while the clump undergoes self-annihilation it emits a GW signal. The high density around the SMBH will be replenished for about  $10^8$  yr, yielding continued GW and

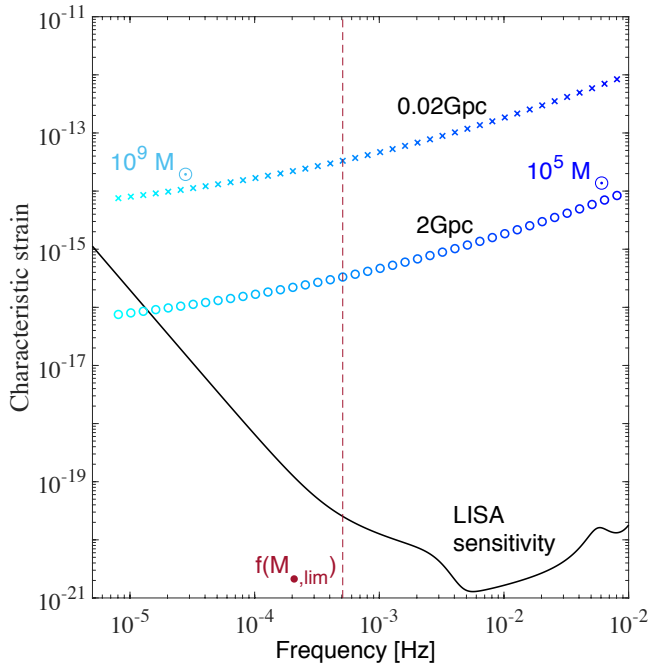


FIG. 3. **Examples for GW signal in LISA band.** We consider 4 yr observational window for source at 0.02 Gpc and 2 Gpc, top crosses and bottom circles, respectively. We consider a range of SMBH masses from  $10^9 M_\odot$  (cyan, left), to  $10^5 M_\odot$ , (blue, right). Over-plotted is the LISA sensitivity curve [56]. If DM self-annihilates, we find a limiting mass,  $M_{\bullet, \text{lim}}$ , (corresponding to a maximum GW frequency) that can sustain the self-gravitating densities. We over-plot the corresponding GW frequency of this mass (dashed red line).

electromagnetic signals.

We note that the accumulation of DM particles due to the EKL mechanism results in a clump that does not have a spherical distribution around the SMBH. Thus, the actual waveform of such a signal is rather complicated and depends on the orbital dynamics of a test particle in a strong gravitational field [34]. We therefore estimate the dimensionless characteristic strain for a circular orbit, which represents the order-of-magnitude of the expected signal [57].

The GW frequency  $f$  of a circular orbit is twice the orbital frequency, and the dimensionless characteristic strain is [55]

$$h_c(a, f) = 2h_0(a, f)fT_{\text{obs}}, \quad (10)$$

where  $T_{\text{obs}}$  is the observation time window and  $h_0(a, f)$  is defined as

$$h_0(a) = \sqrt{\frac{32}{5}} \frac{G^2}{c^4} \frac{m_1 m_2}{D_l a}, \quad (11)$$

where  $D_l$  is the luminosity distance and  $a$  is the semi-major axis of the two objects. Below we adopt  $a = R_{\text{min}}$ . Note that these calculations do not include the spin of the

SMBH, they are order of magnitude consistent with the latest implementation of the analytical model of Extreme Mass-Ratio Inspirals (EMRI) that does include the spin of a SMBH for point mass inspiral [58, 59].

Since the EKL mechanism yields an influx of DM particles for about  $10^8$  yrs (Figure 2), we can consider a long observational window with LISA. Figure 3 depicts the GW signal for two example sources observed for  $T_{\text{obs}} = 4$  yr. The first is located 2 Gpc away and the other located 0.02 Gpc from us. We consider a range of SMBH masses (from  $10^5 M_\odot$ , to the right, to  $10^9 M_\odot$  to the left). As can be seen in the Figure, LISA will be sensitive to a large range of the SMBH mass parameter space, as well as to distant sources.

One may consider an observational window proportional to the annihilation time-scale. This time-scale covers a large range, from about a month ( $\sim 30$  d, for  $10^9 M_\odot$ ) to less than a minute for the low mass SMBHs. This short time-scale is still within the LISA sensitivity window. It is unclear how LISA will handle very short observational windows. However, as mentioned above, we expect a continuous accumulation of DM in the ergosphere, thus, short time-scales, which may be associated with burst-like signals, are less probable.

## V. DISCUSSION

We have shown that, thanks to the EKL mechanism, in SMBH binaries, a self-gravitating DM clump may exist near the ergosphere of a spinning SMBH. DM may accumulate there, over long time-scales allowing for replenishing the possibly self-annihilating DM particles. The mass of the clump can be high enough to allow for a GW signal, detectable by LISA. Our results suggest that this GW signal will be accompanied with high energy electromagnetic signal, from possible DM self-annihilation process.

Note that if the DM does not self-annihilate into particles with detectable signatures, as is the case for gravitinos, DM particles may accumulate to extreme masses in the close vicinity of the SMBH. Some of them may accrete onto the SMBH, however, the high mass clump around the SMBH may result in, for example, gravitino decay products [60]. Moreover, the GW signal in such a case may be even stronger, as the accumulating mass will only increase.

SMBH binaries are a natural consequence of galaxy formation, consistent with observations [61]. We therefore expect that not only the torus-like DM distribution will be a generic outcome of SMBH binaries [30], but also have a GW signal from self-gravitating DM that accumulates in the close vicinity of the SMBH. If DM self-annihilates, we predict that the GW signal will also be accompanied by a high-energy signal.

*Acknowledgments*—SN and JS thank the UCLA Bhau-mik Institute for Theoretical Physics for the hospitality that enabled the completion of this project. SN

acknowledges the partial support of NASA grant No. 80NSSC19K0321, and also thanks Howard and Astrid

Preston for their generous support. JS acknowledges discussions with Enrico Barausse.

- 
- [1] T. Di Matteo, V. Springel, and L. Hernquist, *Nature* **433**, 604 (2005), astro-ph/0502199.
- [2] P. F. Hopkins, L. Hernquist, T. J. Cox, T. Di Matteo, B. Robertson, and V. Springel, *ApJS* **163**, 1 (2006), astro-ph/0506398.
- [3] B. Robertson, J. S. Bullock, T. J. Cox, T. Di Matteo, L. Hernquist, V. Springel, and N. Yoshida, *ApJ* **645**, 986 (2006), astro-ph/0503369.
- [4] S. Callegari, L. Mayer, S. Kazantzidis, M. Colpi, F. Governato, T. Quinn, and J. Wadsley, *ApJ-Lett* **696**, L89 (2009), arXiv:0811.0615.
- [5] A. Sillanpaa, S. Haarala, M. J. Valtonen, B. Sundelius, and G. G. Byrd, *ApJ* **325**, 628 (1988).
- [6] C. Rodriguez, G. B. Taylor, R. T. Zavala, A. B. Peck, L. K. Pollack, and R. W. Romani, *ApJ* **646**, 49 (2006), astro-ph/0604042.
- [7] S. Komossa, H. Zhou, and H. Lu, *ApJ-Lett* **678**, L81 (2008), arXiv:0804.4585.
- [8] T. Bogdanović, M. Eracleous, and S. Sigurdsson, *ApJ* **697**, 288 (2009), arXiv:0809.3262.
- [9] T. A. Boroson and T. R. Lauer, *Nature* **458**, 53 (2009), arXiv:0901.3779 [astro-ph.GA].
- [10] M. Dotti, C. Montuori, R. Decarli, M. Volonteri, M. Colpi, and F. Haardt, *MNRAS* **398**, L73 (2009), arXiv:0809.3446.
- [11] D. Batcheldor, A. Robinson, D. J. Axon, E. S. Perlman, and D. Merritt, *ApJ* **717**, L6 (2010), arXiv:1005.2173 [astro-ph.CO].
- [12] R. P. Deane, Z. Paragi, M. J. Jarvis, M. Coriat, G. Bernardi, R. P. Fender, S. Frey, I. Heywood, H.-R. Klöckner, K. Grainge, and C. Rumsey, *Nature* **511**, 57 (2014), arXiv:1406.6365.
- [13] X. Liu, Y. Shen, F. Bian, A. Loeb, and S. Tremaine, *ApJ* **789**, 140 (2014), arXiv:1312.6694.
- [14] J. Liu, M. Eracleous, and J. P. Halpern, *The Astrophysical Journal* **817**, 42 (2016).
- [15] Y.-R. Li, J.-M. Wang, L. C. Ho, K.-X. Lu, J. Qiu, P. Du, C. Hu, Y.-K. Huang, Z.-X. Zhang, K. Wang, and J.-M. Bai, *ApJ* **822**, 4 (2016), arXiv:1602.05005.
- [16] K. Bansal, G. B. Taylor, A. B. Peck, R. T. Zavala, and R. W. Romani, *ApJ* **843**, 14 (2017), arXiv:1705.08556.
- [17] P. Kharb, D. V. Lal, and D. Merritt, *Nature Astronomy* **1**, 727 (2017), arXiv:1709.06258.
- [18] J. C. Runnoe, M. Eracleous, A. Pennell, G. Mathes, T. Boroson, S. Sigurdsson, T. Bogdanovc, J. P. Halpern, J. Liu, and S. Brown, *MNRAS* **468**, 1683 (2017), arXiv:1702.05465.
- [19] D. W. Pesce, J. A. Braatz, J. J. Condon, and J. E. Greene, *ApJ* **863**, 149 (2018), arXiv:1807.04598.
- [20] S. Komossa, V. Burwitz, G. Hasinger, P. Predehl, J. S. Kaastra, and Y. Ikebe, *ApJ-Lett* **582**, L15 (2003), astro-ph/0212099.
- [21] S. Bianchi, M. Chiaberge, E. Piconcelli, M. Guainazzi, and G. Matt, *MNRAS* **386**, 105 (2008), arXiv:0802.0825.
- [22] J. M. Comerford, R. L. Griffith, B. F. Gerke, M. C. Cooper, J. A. Newman, M. Davis, and D. Stern, *ApJ-Lett* **702**, L82 (2009), arXiv:0906.3517 [astro-ph.CO].
- [23] X. Liu, J. E. Greene, Y. Shen, and M. A. Strauss, *ApJ-Lett* **715**, L30 (2010), arXiv:1003.3467 [astro-ph.CO].
- [24] P. J. Green, A. D. Myers, W. A. Barkhouse, J. S. Mulchaey, V. N. Bennert, T. J. Cox, and T. L. Aldcroft, *ApJ* **710**, 1578 (2010), arXiv:1001.1738 [astro-ph.GA].
- [25] K. L. Smith, G. A. Shields, E. W. Bonning, C. C. McMullen, D. J. Rosario, and S. Salviander, *ApJ* **716**, 866 (2010), arXiv:0908.1998.
- [26] J. M. Comerford, R. Nevin, A. Stemo, F. Müller-Sánchez, R. S. Barrows, M. C. Cooper, and J. A. Newman, *ApJ* **867**, 66 (2018), arXiv:1810.11543.
- [27] M. C. Begelman, R. D. Blandford, and M. J. Rees, *Nature* **287**, 307 (1980).
- [28] M. Milosavljević and D. Merritt, *ApJ* **563**, 34 (2001), astro-ph/0103350.
- [29] Q. Yu, *MNRAS* **331**, 935 (2002), astro-ph/0109530.
- [30] S. Naoz and J. Silk, *ApJ* **795**, 102 (2014), arXiv:1409.5432.
- [31] S. Naoz, B. Kocsis, A. Loeb, and N. Yunes, *ApJ* **773**, 187 (2013), arXiv:1206.4316 [astro-ph.SR].
- [32] S. Naoz, *ARA&A* **54**, 441 (2016), arXiv:1601.07175 [astro-ph.EP].
- [33] G. Li, S. Naoz, B. Kocsis, and A. Loeb, *ApJ* **785**, 116 (2014), arXiv:1310.6044 [astro-ph.EP].
- [34] C. M. Will and M. Maitra, *Phys. Rev. D* **95**, 064003 (2017), arXiv:1611.06931 [gr-qc].
- [35] F. Ferrer, A. Medeiros da Rosa, and C. M. Will, *Phys. Rev. D* **96**, 083014 (2017), arXiv:1707.06302.
- [36] J. Silk and A. Stebbins, *ApJ* **411**, 439 (1993).
- [37] V. Berezhinsky, V. Dokuchaev, Y. Eroshenko, M. Kachelrieß, and M. A. Solberg, *Phys. Rev. D* **81**, 103529 (2010), arXiv:1002.3444 [astro-ph.CO].
- [38] V. S. Berezhinsky, V. I. Dokuchaev, and Y. N. Eroshenko, *Physics Uspekhi* **57**, 1-36 (2014), arXiv:1405.2204 [astro-ph.HE].
- [39] S. Naoz and R. Narayan, *ApJ* **791**, L8 (2014), arXiv:1407.3795.
- [40] C. Popa, S. Naoz, F. Marinacci, and M. Vogelsberger, *MNRAS* **460**, 1625 (2016), arXiv:1512.06862.
- [41] Y. S. Chiou, S. Naoz, F. Marinacci, and M. Vogelsberger, *MNRAS* **481**, 3108 (2018), arXiv:1809.05097.
- [42] Y. S. Chiou, S. Naoz, B. Burkhardt, F. Marinacci, and M. Vogelsberger, *arXiv e-prints* (2019), arXiv:1904.08941.
- [43] E. W. Kolb and I. I. Tkachev, *Phys. Rev. D* **50**, 769 (1994), astro-ph/9403011.
- [44] A. A. Starobinskij, *Soviet Journal of Experimental and Theoretical Physics Letters* **55**, 489 (1992).
- [45] E. Bertschinger, *ApJS* **58**, 39 (1985).
- [46] P. Gondolo and J. Silk, *Physical Review Letters* **83**, 1719 (1999), arXiv:astro-ph/9906391.
- [47] T. Lacroix, C. BÅhlm, and J. Silk, *Phys. Rev. D* **89**, 063534 (2014), arXiv:1311.0139 [astro-ph.HE].
- [48] T. Lacroix and J. Silk, *ApJ* **853**, L16 (2018), arXiv:1712.00452.
- [49] Y. Ali-Haïmoud, E. D. Kovetz, and J. Silk, *Phys. Rev. D* **93**, 043508 (2016), arXiv:1511.02232 [astro-ph.HE].

- [50] G. Jungman, M. Kamionkowski, and K. Griest, *Phys. Rep.* **267**, 195 (1996), hep-ph/9506380.
- [51] S. Tremaine, K. Gebhardt, R. Bender, G. Bower, A. Dressler, S. M. Faber, A. V. Filippenko, R. Green, C. Grillmair, L. C. Ho, J. Kormendy, T. R. Lauer, J. Magorrian, J. Pinkney, and D. Richstone, *ApJ* **574**, 740 (2002), astro-ph/0203468.
- [52] C. Boehm and J. Lavalle, *Phys. Rev. D* **79**, 083505 (2009).
- [53] We note that we have tested a larger value as well, which slightly changed the total accumulated mass but did not affect the overall, qualitative conclusion.
- [54] G. Li, S. Naoz, B. Kocsis, and A. Loeb, *MNRAS* **451**, 1341 (2015), arXiv:1502.03825.
- [55] P. C. Peters, *Physical Review* **136**, 1224 (1964).
- [56] T. Robson, N. Cornish, and C. Liu, arXiv e-prints (2018), arXiv:1803.01944 [astro-ph.HE].
- [57] E. Barausse, V. Cardoso, and P. Pani, *Phys. Rev. D* **89**, 104059 (2014), arXiv:1404.7149 [gr-qc].
- [58] A. J. K. Chua and J. R. Gair, *Classical and Quantum Gravity* **32**, 232002 (2015), arXiv:1510.06245 [gr-qc].
- [59] A. J. K. Chua, C. J. Moore, and J. R. Gair, *Phys. Rev. D* **96**, 044005 (2017), arXiv:1705.04259 [gr-qc].
- [60] M. Grefe, in *Journal of Physics Conference Series*, Journal of Physics Conference Series, Vol. 375 (2012) p. 012035, arXiv:1111.7117 [hep-ph].
- [61] R. S. Barrows, J. M. Comerford, and J. E. Greene, *ApJ* **869**, 154 (2018), arXiv:1811.01973.